



ICA 2013 Montreal

Montreal, Canada

2 - 7 June 2013

Engineering Acoustics

Session 1aEA: Thermoacoustics I

1aEA2. Finite element simulation of a two-dimensional standing wave thermoacoustic engine

Jan A. De Jong*, Ysbrand H. Wijnant and André De Boer

***Corresponding author's address: Engineering Technology, University of Twente, P.O. Box 217, Enschede, 7500AE, Overijssel, Netherlands, j.a.dejong@utwente.nl**

Thermoacoustic engines use heat to produce acoustic power. The subject of this manuscript is modeling of thermoacoustic engines. A finite element simulation has been performed on a theoretical example of a two-dimensional standing wave thermoacoustic engine. The simulation solves the linearized Navier-Stokes equations in the frequency domain. The analysis is used to obtain the (thermo)acoustic eigenfrequencies and the corresponding mode shapes of the engine. The nonlinear eigenfrequency problem is solved using an iterative (modified) Newton-Raphson method. The engine starts to oscillate (onset) when a linear instability is present. An instability can be determined when the imaginary part of an eigenfrequency of the engine crosses zero and becomes negative.

Published by the Acoustical Society of America through the American Institute of Physics

INTRODUCTION

Thermoacoustic (TA) engines are heat engines which convert heat into acoustic power. The acoustic power can be converted to useful electricity by means of an electro-acoustic energy transducer, such as a linear alternator. The established theory for the design and modeling of thermoacoustic systems is the one developed by Swift et al [1], based on the linear thermoacoustic theory of Rott et al [2]. This essentially 1D theory is implemented in the program DELTAEC [3], which is widely used as a design tool for thermoacoustic systems. The theory is valid when a significant distinction can be made between the wave propagation direction and the direction perpendicular to it (the cross-direction). In most cases, prismatic tubes are considered with a typical cross-section length scale (i.e. the hydraulic radius) which is much smaller than the acoustic wavelength. However, for accurate modeling of curved tubes, changes in cross-sectional area, etc., a more-dimensional analysis is required. Hence, for the design of diverse and compact thermoacoustic engine geometries, a 3D linear thermoacoustic model is developed. With this model, stability analyses of actual thermoacoustic engine geometries can be performed. In this paper, the implementation such a theory is illustrated by means of a 2D standing wave (noise generating) TA engine.

MODEL

The model is based on linearization of the governing equations, i.e. the continuity, momentum and energy equation accompanied with a suitable equation of state. We consider only the fluid domain, and in this case, Fourier-Newtonian perfect gas behavior is assumed. Body forces are neglected, and furthermore it is assumed that the fluid is in mechanical equilibrium, so no mean flow is present. The fluid is heated with a hot heat exchanger and kept cool with a cold one. The heat exchanger surface in contact with the fluid domain is assumed to be isothermal, so the heat input at the hot heat exchangers is roughly proportional to the temperature difference between the hot and the cold heat exchanger; this creates a non-isothermal fluid domain. The temperature field in the fluid can be obtained by solving the heat equation,

$$\nabla \cdot (\kappa_m \nabla T_m) = 0, \quad (1)$$

with the boundary conditions $T_m = T_w$ at boundary Γ_w and $-\kappa_m \nabla T_m = \mathbf{0}$ at Γ_{ad} . κ_m denotes the (mean temperature dependent) thermal conductivity of the fluid and T_m the mean temperature. When the heat equation is solved, a mean temperature field is obtained, from which the mean density field is computed using the ideal gas law (the mean pressure is constant throughout the domain). For the stability analysis, we look at small deviations (perturbations) from equilibrium. The perturbations are considered so small, that they do not influence the mean field. The model equations for these small perturbations, including thermal and viscous effects, are the inhomogeneous Fourier transformed Linearized Navier-Stokes (FLNS) equations. The FLNS equations were derived in earlier work [4], where a homogeneous quiescent mean field was assumed. Thermoacoustic effects are included when the mean temperature and density fields are non-constant. The terms corresponding to the inhomogeneous field are added to the FLNS equations. The 'extended' Fourier transformed acoustic continuity, momentum and enthalpy

equations then become:

$$i\omega \left(\frac{p_1}{\rho_m} - \frac{T_1}{T_m} \right) + \nabla \cdot \mathbf{u}_1 - \frac{\mathbf{u}_1 \cdot \nabla T_m}{T_m} = 0 \quad (2a)$$

$$i\omega \rho_m \mathbf{u}_1 + \nabla p_1 = \nabla \cdot \underline{\boldsymbol{\tau}}_1, \quad (2b)$$

$$\rho_m c_p (i\omega T_1 + \mathbf{u}_1 \cdot \nabla T_m) - i\omega p_1 = \nabla \cdot (\kappa_m \nabla T_1) \quad (2c)$$

A detailed derivation is given in [5]. p denotes the pressure, \mathbf{u} the velocity and T the temperature. Subscript m denotes mean (time-invariant) quantities. In addition, the phasor notation of Swift [1] is adopted: $\xi'(\mathbf{x}, t) = \Re(\xi_1 e^{i\omega t})$. Where ξ' is one of the fluctuations ρ' , p' or \mathbf{u}' . Note that the gas law has been used to replace the gradient of the density with the gradient of the temperature. $\underline{\boldsymbol{\tau}}_1$ denotes the acoustic viscous stress tensor:

$$\underline{\boldsymbol{\tau}}_1 = \mu_m \left(\nabla \mathbf{u} + (\nabla \mathbf{u})^T - \frac{2}{3} \mu_m (\nabla \cdot \mathbf{u}) \mathbf{I} \right) + \mu_B (\nabla \cdot \mathbf{u}) \mathbf{I} \quad (3)$$

Here, μ_m denotes the mean dynamic viscosity and μ_B the bulk viscosity. To solve the system of equations [2], a weak formulation is derived:

$$\int_{\Omega} p_w \left(i\omega \left(\frac{p_1}{\rho_m} - \frac{T_1}{T_m} \right) + \nabla \cdot \mathbf{u}_1 - \frac{\mathbf{u}_1 \cdot \nabla T_m}{T_m} \right) d\Omega = 0, \quad (4a)$$

$$\int_{\Omega} (i\omega \rho_m \mathbf{u}_1 \cdot \mathbf{u}_w + \underline{\boldsymbol{\tau}}_1 : \nabla \mathbf{u}_w - p_1 \nabla \cdot \mathbf{u}_w) d\Omega = \int_{\Gamma} \mathbf{t}_1 \cdot \mathbf{u}_w d\Gamma, \quad (4b)$$

$$\int_{\Omega} [T_w (\rho_m c_p (i\omega T_1 + \mathbf{u}_1 \cdot \nabla T_m) - i\omega p_1) + \nabla T_w \cdot (\kappa_m \nabla T_1)] d\Omega = - \int_{\Gamma} T_w \mathbf{q}_1 \cdot \mathbf{n} d\Gamma, \quad (4c)$$

where subscript w denotes the weighting function. Note that the natural boundary conditions as they result from partial integration are put on the right hand side. They comprise the normal traction (\mathbf{t}_1) for the momentum equation and the normal acoustic heat flux ($\mathbf{q}_1 \cdot \mathbf{n}$) for the energy equation. If equations 4 are true for all weighting functions, then equations 2 are satisfied. In the finite element method however, the equations are not satisfied for all weighting functions, but only for a limited number. In this case, the Galerkin method is chosen, so the weighting function basis is chosen to be equal to the basis functions of the dependent variables [6]. The weak formulations are implemented in the commercial software package Comsol Multiphysics [7]. Once a choice is made for the interpolation functions, the system of equations can be assembled. For a given frequency and mean temperature field, a linear system of equations is obtained.

Solution method

With equations 2, two types of analyses can be done: a frequency response analysis and an eigenfrequency analysis. The last one is of interest for thermoacoustic engines, since a thermoacoustic engine is not “driven” at a certain frequency, but starts when a linear instability arises.

As mentioned before, the resulting algebraic system from weak formulations 4 is linear. However, the eigenfrequency problem can still become nonlinear when an analysis has to be done with nonlinear frequency dependent impedance boundary conditions. An example of such a boundary condition is an acoustic open end from which sound is radiated. Because the impedance at the open end is a nonlinear function of the frequency, the eigenfrequency problem becomes nonlinear as well. To deal with this inconvenience, the problem is not solved as a regular eigenvalue problem. Instead, we apply a unit acoustic pressure (the unit pressure scales the mode) at the open end and calculate the impedance at the open end from the finite element result (Z_{FEM}). The

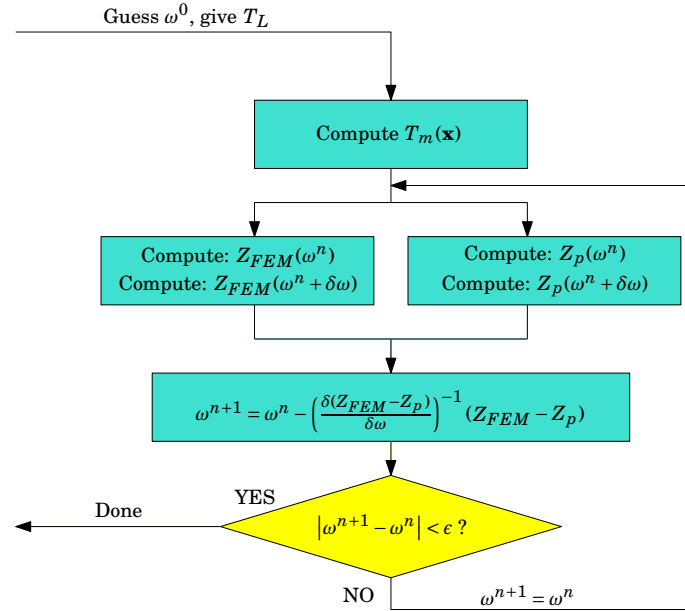


FIGURE 1: Flow chart to obtain the solution of the nonlinear eigenfrequency problem.

resulting impedance is compared with the required radiation impedance (Z_p). A modified Newton-Raphson solution technique is used to solve the frequency for which the calculated impedance matches the radiation impedance. It is modified in the sense that the Jacobian matrix $\partial(Z_{FEM} - Z_p)/\partial\omega$ is estimated with forward Euler finite differences. The difference $\delta\omega$ is chosen as 5% the convergence criterium (ϵ). Convergence is reached when the absolute difference between the updated frequency and the current frequency is smaller than 10^{-3} rad/s. A flowchart of the iterative scheme is shown in figure 1.

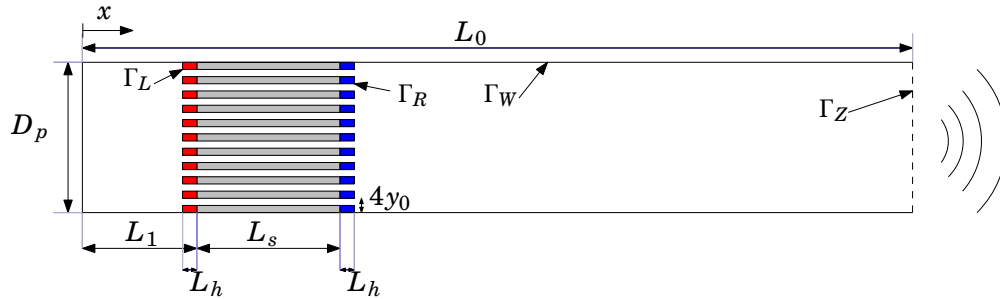
The resulting eigenfrequencies are complex and the imaginary part of the eigenfrequency is a measure for the damping of the eigenmode, since: $e^{i\omega t} \equiv e^{-\Im(\omega)t} \cdot e^{i\Re(\omega)t}$. Hence, a negative imaginary part of the eigenfrequency results in an unstable (thermo)acoustic eigenmode. The eigenfrequencies change when a different mean temperature field is applied.

EXAMPLE: 2D STANDING WAVE ENGINE

Figure 2 shows a 2D standing wave engine. The dimensions are listed in table 1. When sufficient heat is added at the hot heat exchangers (the red part), the first (thermo)acoustic eigenmode becomes unstable. The acoustic medium is air, so a 3D variant of this engine will typically run with a dominating oscillation frequency close to $c_0/4L_0$. Where c_0 is the ambient speed of sound (≈ 340 m/s) at the reference temperature (20°C) and L_0 is the length of the engine. We are interested in the thermoacoustic eigenmodes of this engine, as a function of the hot temperature boundary condition of the stack. Table 2 shows an overview of the different boundaries with their corresponding boundary conditions. The sound is radiated from the right side (acoustic open end), where a radiation impedance of a baffled piston is applied [8]. At all other walls, the no-slip boundary condition is applied for the acoustic velocity. The acoustic temperature fluctuation is assumed to be zero at the walls. We are interested in the first two eigenmodes of the system. The starting value for the Newton Raphson method is chosen close to the eigenfrequency, in this case, since L_0 is 0.17 m: $f_1 \approx 500$ Hz, $f_2 \approx 1500$ Hz. A mesh study has been performed to determine the

TABLE 1: Dimensional parameters of the 2D standing wave engine

Parameter	Value	Parameter	Value
L_0	17 cm	L_1	3 cm
L_s	1.5 cm	L_h	0.15 cm
W_0	2.1 cm	y_0	0.5 mm
ϕ	10/21		

**FIGURE 2:** Schematic of the 2D standing wave engine including dimensional parameters

required mesh size. The final mesh is chosen such that the results become nearly mesh-independent. Since the problem is only 2D, the velocity vector comprises only the x- and y-velocity.

Results

Figure 3 shows the real part of the acoustic pressure of the first and second mode corresponding to the mean temperature distribution with $T_L = 100^\circ\text{C}$ on Γ_L and T_R at 20°C on Γ_R . Due to the boundary condition at the open end where the pressure phase is set to 0° , i.e., $p_1 = 1 + 0i$ Pa, this figure shows the instantaneous acoustic pressure at the time $t = 0$. The mode shapes correspond very well with the expected $\lambda/4$ and $3\lambda/4$ mode shapes respectively. Figure 4 shows the velocity profile at the first eigenfrequency in the engine. Two cross sections are taken. One in the stack from $y = 0$ to $y = W_0$ and one across the whole engine from $x = 0$ to $x = L_0$. The cross-velocity profile closely resembles the expected analytic hyperbolic cosine function result [1]. Due to the decrease in porosity, the acoustic velocity in the stack is higher than in the resonator parts, roughly proportional to the inverse of the porosity. In figure 5, the imaginary part of the eigenfrequency (scaled with the magnitude of the eigenfrequency) is plotted against temperature T_L in the system, keeping the temperature T_R constant (20°C). At $T_L \approx 250^\circ\text{C}$, $\Im(\omega)$ of the first mode crosses zero. Therefore, we expect oscillation onset at this temperature difference. The second mode shows a slow trend to get more unstable at a higher temperature. However in the calculated temperature range, this mode stays stable. The calculated mean temperature gradient in the stack varies between

TABLE 2: Boundary conditions for the 2D standing wave engine

	Γ_L	Γ_R	Γ_W	Γ_Z
Mean temperature	$T_m = T_L$	$T_m = T_R$	$\mathbf{q}_m \cdot \mathbf{n} = 0$	$\mathbf{q}_m \cdot \mathbf{n} = 0$
Acoustic velocity	$\mathbf{u}_1 = \mathbf{0}$	$\mathbf{u}_1 = \mathbf{0}$	$\mathbf{u}_1 = \mathbf{0}$	free
Acoustic temperature	$T_1 = 0$	$T_1 = 0$	$T_1 = 0$	$\mathbf{q}_1 \cdot \mathbf{n} = 0$
Acoustic pressure	free	free	free	$p_1 = 1$ Pa

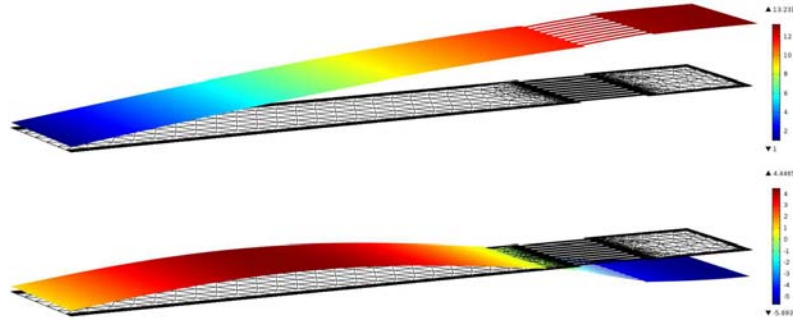


FIGURE 3: Real part of the pressure distribution of the first (above) and second eigenmode (below) of the 2D standing wave engine. At the $p_1 = 0$ plane, the mesh is plotted.

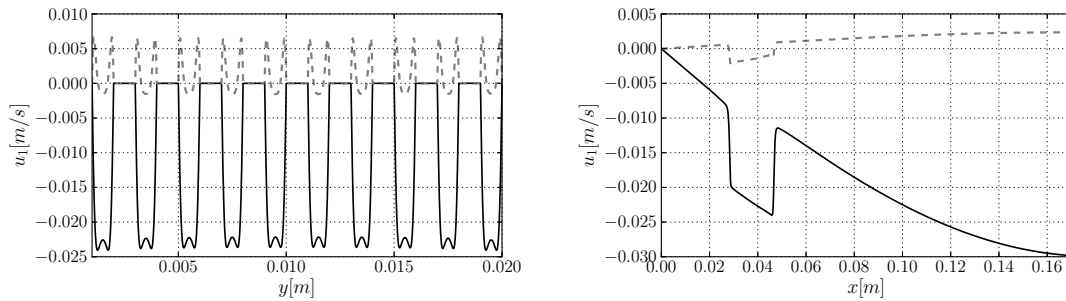


FIGURE 4: x-velocity profile of the first eigenmode plotted as a function of the y-coordinate in the stack (left) at $x = L_1 + \frac{1}{2}L_s$, and as a function of the x-position in the resonator at $y = 11/21 \cdot W_0$ (right). (---) = $\Re(u_1)$; (—) = $\Im(u_1)$

$-8.0 \cdot 10^3$ and $-6.7 \cdot 10^3$ K/m. It is slightly nonlinear in the x-direction due to the temperature dependent thermal conductivity. In this study, the transverse heat conduction between the stack material and the acoustic medium is neglected by the application of the zero normal heat flux boundary condition. Therefore, it is noted that this mean temperature field deviates more from a linear temperature profile than in a real stack.

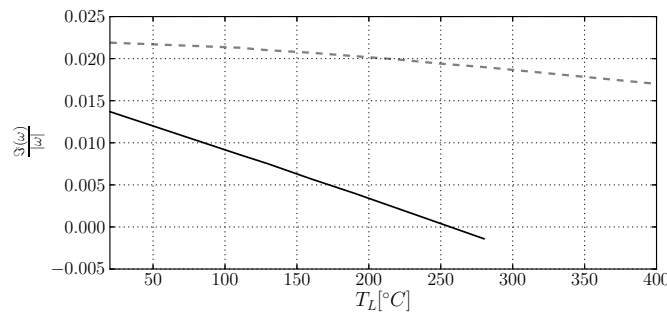


FIGURE 5: Scaled imaginary part of the eigenfrequency vs hot temperature for the first two eigenmodes: (—) $\lambda/4$ mode; (---) $3\lambda/4$ mode.

CONCLUSIONS AND FUTURE WORK

A stability analysis of a thermoacoustic system can be performed using the finite element method. The method is applied to compute the eigenfrequency as a function of the temperature distribution for two eigenmodes of a 2D standing wave engine. The geometry of this 2D standing wave engine is chosen such that the 1D theory still yields accurate results, so a comparison can be made. A verification of the current finite element implementation is shown in [5], including a method to compute the stability limit. The stability limit is the precise amount of heating to obtain self-sustained oscillations. Future work will involve the expansion of the current theory to second order. This allows the computation of (weakly) nonlinear effects. Furthermore, the saturation amplitude, acoustic power production, as well as second order acoustic streaming patterns will be calculated.

ACKNOWLEDGMENTS

This research has been carried out as a part of the Agentschap NL EOS-KTO (KTOT03009) research program. The financial support is gratefully acknowledged.

REFERENCES

- [1] G. W. Swift, "Thermoacoustics: A unifying perspective for some engines and refrigerators", *The Journal of the Acoustical Society of America* **113**, 2379 (2003).
- [2] N. Rott, "Damped and thermally driven acoustic oscillations in wide and narrow tubes", *Zeitschrift für angewandte Mathematik und Physik ZAMP* **20**, 230–243 (1969).
- [3] W. C. Ward and G. W. Swift, "Design environment for low-amplitude thermoacoustic engines", *The Journal of the Acoustical Society of America* **95**, 3671–3672 (1994).
- [4] W. R. Kampinga, *Viscothermal acoustics using finite elements: analysis tools for engineers* (University of Twente) (2010).
- [5] J. A. de Jong, Y. H. Wijnant, and A. de Boer, "Stability analysis of thermoacoustic engines using the finite element method", (2013), to be published.
- [6] J. van Kan, A. Segal, and F. Vermolen, *Numerical methods in scientific computing (VSSD)* (2008).
- [7] "COMSOL multiphysics finite element programming environment", (2012), <http://www.comsol.com/>.
- [8] D. Blackstock, *Fundamentals of physical acoustics* (Wiley-interscience) (2000).